

# Numerical Simulation of Compact U(1) Lattice Gauge Theory

KOMA Yoshiaki \*

**Abstract:** Compact U(1) lattice gauge theory possesses a confinement phase, which can be regarded as a prototype of quantum chromodynamics QCD for describing strong interaction of quarks and gluons. We revisit this theory and perform Monte Carlo simulations to gain idea on the structure of the nonperturbative QCD vacuum.

Key Words: Compact U(1) lattice gauge theory, Lattice QCD simulations

## 1. Introduction

Clarifying nonperturbative properties of quantum chromodynamics (QCD), a gauge field theory of SU(3) group symmetry for describing strong interaction of quarks and gluons, remains an important topic in hadron physics. Monte Carlo simulations of QCD defined on a discrete spacetime, referred to as the lattice QCD simulations, offer a powerful tool for this purpose, which in principle make it possible for us to compute directly the expectation values of physical quantities involving nontrivial quantum effects. The problems are, however, that the numerical simulations usually require a lot of computer resources for reducing numerical errors, and the numerical result itself is not enough to understand the underlying physical mechanism, even if one successfully obtains very precise numerical values. In this respect, complementary studies are always useful to get an insight into the true nature of nonperturbative QCD.

One of the mysterious phenomena that could be explained by nonperturbative QCD is the fact that one never observe an isolated quark in the accelerator experiment, which means that the quarks are somehow confined inside hadrons. This is called the quark confinement problem, and is not yet satisfactorily solved. For this problem the lattice QCD simulations provide us with a numerical answer. The static potential extracted from the expectation value of the Wilson loop shows that the functional form of the potential consists of a Coulombic term and a linearly rising term as a function of the distance between the quark and the antiquark. Although what kind of mechanism determines the functional form is not clarified, the linear term can explain why a single quark cannot be isolated with a finite amount of energy.

A plausible idea on the mechanism is that the QCD vacuum acts as a dual superconductor for the color-electric field associated with the quarks. In fact, the static potential of the classical flux-tube solution in the dual Ginzburg-Landau (DGL) theory exhibits a similar functional form [1], where the physical mechanism in this effective theory originates from the dual Meissner effect. The static potential for the three quarks that we have successfully obtained by the lat-

tice QCD simulations [2] also supports the dual superconductor picture of the QCD vacuum. However, it is as yet nontrivial why QCD has a property like a dual superconductor. If this is the true nature of nonperturbative QCD, the theory should be connected theoretically with the DGL theory.

In this report, we revisit numerical simulations of the compact U(1) lattice gauge theory (U(1) LGT) [3, 4]. This theory is not exactly the same as QCD, but can be regarded as a small laboratory of QCD as it possesses a confinement phase. In addition, the reduction of gauge degrees of freedom drives down the cost of simulations, allowing for computing various quantities. In the confinement phase, many direct evidence of supporting the dual superconductor picture have been found so far. The observed profile of the electric field between a positive and a negative electric charges has a one-dimensional flux tube shape, accompanied by circulating monopole supercurrent [5], which means that the dual Meissner effect clearly occurs. Therefore, detailed comparisons with the U(1) LGT results with those of the DGL theory from various points of view may give us some hints for the theoretical connection between QCD and the DGL theory.

## 2. Numerical procedure

Given an action of the theory  $S[\phi]$  of field variables  $\phi$ , the expectation value of a quantum operator  $O(\phi)$  is schematically computed as

$$\langle O \rangle = \int D\phi O(\phi) e^{-\beta S[\phi]}, \quad (1)$$

where the value  $\beta$  controls the strength of interaction, corresponding to the inverse temperature in statistical mechanics. In practice, we define the theory on a discrete lattice of spacetime and generate a sequence of independent field configurations  $\{\phi_i\}$  with the Boltzmann weight of  $\exp(-\beta S[\phi])$  by the Monte-Carlo method. We then evaluate the average of the operator for the number of configurations  $N_{\text{conf}}$ , which finally reduces to the expectation value  $\langle O \rangle$  by taking the limit  $N_{\text{conf}} \rightarrow \infty$ . This is the basic methodology of the lattice simulations. Of course, it is impossible to prepare infinite number of the field configurations with infinite lattice volume with infinitesimal lattice spacing, and hence statistical and systematic errors of the numerical results need to be controlled properly.

---

\*Division of Liberal Arts

In the U(1) LGT, the action consists of link variables (variables between two nearest sites) defined by  $U_\mu(m) = \exp(i\theta_\mu(m)) \in \text{U}(1)$ , where  $\mu$  and  $m$  denote a direction and a site labels. The link variables are compact as they are unchanged under the transformation  $\theta_\mu \rightarrow \theta_\mu + 2\pi n_\mu$  with an integer  $n_\mu$ . The most simple action of the U(1) LGT is called the Wilson gauge action of the form

$$S[U] = \sum_{m, \mu < \nu} S_{\mu\nu}(m) = \sum_{m, \mu < \nu} \{1 - \text{Re } U_{\mu\nu}(m)\}, \quad (2)$$

where  $U_{\mu\nu}(m) = U_\mu(m)U_\nu(m + \hat{\mu})U_\mu^\dagger(m + \hat{\nu})U_\nu^\dagger(m)$  are called the plaquette variables. We consider four dimensional spacetime with the lattice volume  $V = L^3T$ , where  $L$  and  $T$  are the space and time extents of the lattice, and impose periodic boundary conditions in all directions. The number of link variables is  $N_{\text{link}} = 4L^3T$ . A sequence of independent link variables is generated by using a mixture of heatbath (HB) and over-relaxation (OR) methods. In the weak coupling limit as  $\beta \rightarrow 0$ , the action reduces to the continuum action for the field strength part of quantum electrodynamics (QED).

### 3. Numerical results

In order to test the validity of our OpenMP code with double precision arithmetic, we first compute the average action per plaquette  $\langle E \rangle = \langle S \rangle / N_{\text{plaq}}$  (expectation value of the action density) on a  $16^4$  lattice as in the works [3, 4], where an update of link variables is achieved by 1 HB followed by 3 OR. The number of plaquette variables is  $N_{\text{plaq}} = 6L^3T$ . In Fig. 1, we plot the result as a function of the  $\beta$  values. Each data point is given by the average of  $N_{\text{conf}} = 50$  configurations, which are separated by 100 updates. We obtain the same result as in [3, 4], supporting the validity of our setup. The present result is obtained by using the Mac mini (2018). The phase transition occurs around  $\beta \simeq 1.01$ . In order to achieve an efficient link update, we have checked the acceptance ratio (ACR) in advance as a function of the trial numbers  $N_{\text{hit}}$  as in Fig. 2, and then decided to take  $N_{\text{hit}} = 4$ , which guarantees that about 95% of whole link variables are replaced by the new ones in 1 HB process.

We next examine the probability density function (PDF) of the action current density and its relation to the monopole current [6]. We construct the Abelian plaquette variables from the phase of the link variables as

$$\theta_{\mu\nu}(m) = \theta_\mu(m) + \theta_\nu(m + \hat{\mu}) - \theta_\mu(m + \hat{\nu}) - \theta_\nu(m), \quad (3)$$

and decompose this into a regular part  $\bar{\theta}_{\mu\nu} \in [-\pi, \pi)$  and a singular part  $n_{\mu\nu}(m) = 0, \pm 1, \pm 2$  as  $\theta_{\mu\nu}(m) = \bar{\theta}_{\mu\nu} + 2\pi n_{\mu\nu}(m)$ . The boundary of  $n_{\mu\nu}(m)$  is then identified as the monopole current

$$k_\mu(m_d) = -\frac{1}{2} \epsilon_{\mu\nu\rho\sigma} \partial_\nu n_{\rho\sigma}(m + \hat{\mu}), \quad (4)$$

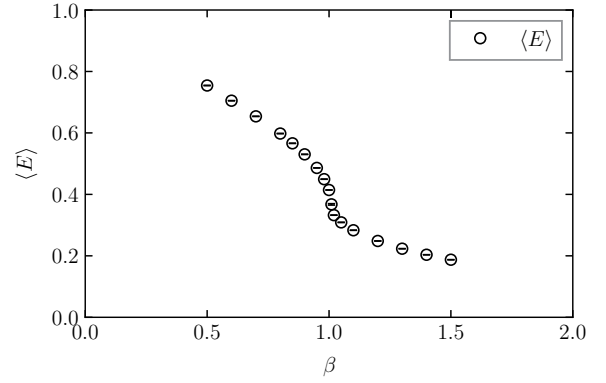


Fig. 1: The average action per plaquette  $\langle E \rangle$  as a function of  $\beta$  values on a  $16^4$  lattice.

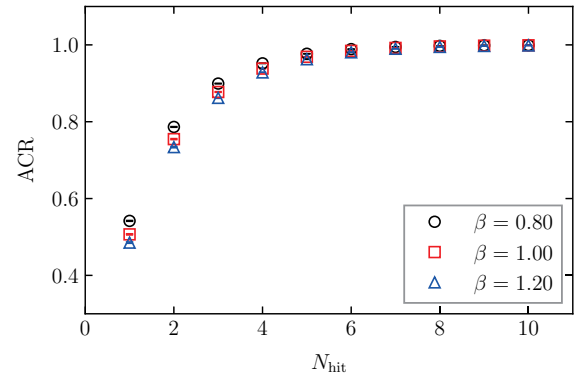


Fig. 2: The acceptance ratio (ACR) of link variables (average of 80 updates) as a function of the trial numbers  $N_{\text{hit}}$  at  $\beta = 0.80, 1.00$ , and  $1.20$  on a  $16^4$  lattice.

where  $m_d = m + (\hat{1} + \hat{2} + \hat{3} + \hat{4})/2$  denotes a dual site. We define the action current density on the dual links so as to be comparable with the location of monopole current such as

$$S_\mu(m_d) = \frac{1}{12} |\epsilon_{\mu\alpha\beta\gamma}| (S_{\alpha\beta}(m + \hat{\mu}) + S_{\alpha\beta}(m + \hat{\mu} + \hat{\gamma})). \quad (5)$$

Note that this satisfies  $\langle \sum_{m_d, \mu} S_\mu(m_d) \rangle / N_{\text{link}} = \langle E \rangle$ . In Fig. 3, we plot the normal PDF and the PDF just on the monopole current on a  $16^4$  lattice, where three  $\beta$  values at 0.80, 1.00 (confinement phase), and 1.20 (deconfinement phase) are selected. We find an interesting behavior in the confinement phase such that the normal PDF is distorted by the presence of monopole current. A remarkable point may be that the peak position of the PDF on the monopole current is insensitive to the change of  $\beta$  values, although the height decreases as the  $\beta$  increases. There is a small peak even at  $\beta = 1.20$  in the deconfinement phase, although its contribution to the PDF is negligible.

We then compute the static potential between a positive and a negative electric charges. A usual

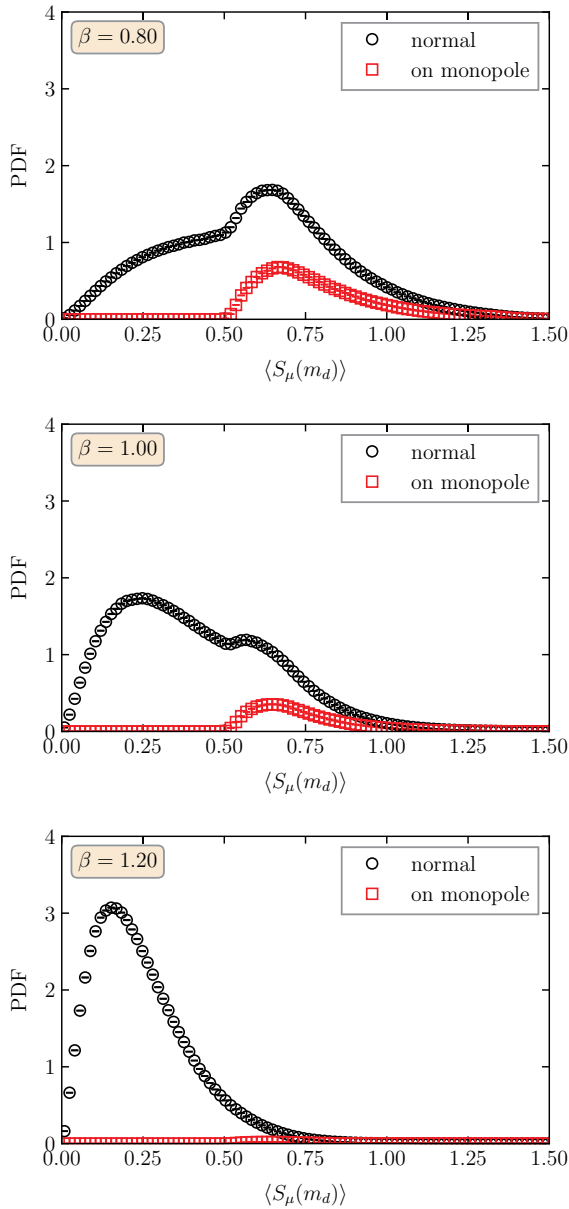


Fig. 3: The probability density function (PDF) of the action current density at  $\beta = 0.80$  (top),  $1.00$  (middle), and  $1.20$  (bottom) on a  $16^4$  lattice. The circle symbols are for the normal action current density, while the square just on the monopole current.

method is to extract it from the expectation value of the Wilson loop, but here, we extract it from the correlation function of the Polyakov loop operator  $P(\vec{m}) = \prod_{t=1}^T U_4(\vec{m}, t)$ , which we call the PLCF, as

$$V(r) = -\frac{1}{T} \ln \langle P(\vec{m}_1) P(\vec{m}_2) \rangle + O(e^{-(\Delta E)T}), \quad (6)$$

where  $r = |\vec{m}_1 - \vec{m}_2|$ . It is important to note that the systematic error is much smaller than that from the Wilson loop once the expectation value of the PLCF is computed accurately.

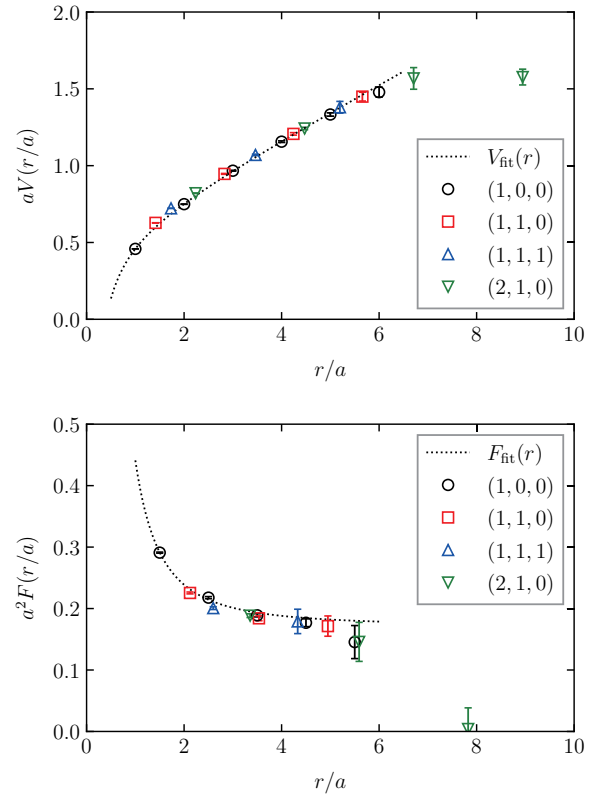


Fig. 4: The static potential (upper) and the force (lower) at  $\beta = 1.00$  on a  $24^4$  lattice for  $N_{\text{tsl}} = 3$  and  $N_{\text{iupd}} = 2000$  with  $N_{\text{conf}} = 20$ . The labels  $(1, 0, 0)$ ,  $(1, 1, 0)$ ,  $(1, 1, 1)$ , and  $(2, 1, 0)$  specify the unit vectors pointing from a positive to a negative charges.

In Ref. [5], we computed the PLCF by using the multilevel algorithm [7] and obtained precise results on a  $16^4$  lattice. The multilevel algorithm is applicable to any lattice gauge theories as long as a local gauge action, such as the Wilson action, is simulated. In this algorithm, the lattice volume is divided into sublattices along the time direction and the parts of operator are simulated with internal updates of link variables, where the spatial links at the boundaries of the sublattices remain intact. The efficient use of the algorithm requires a tune of the temporal size of the sublattice  $N_{\text{tsl}}$  and the number of internal updates  $N_{\text{iupd}}$ . In Ref. [5], we performed simulation with the temporal size of the sublattice  $N_{\text{tsl}} = 2$  within single precision arithmetic.

In the present study, we have examined the temporal size dependence of the numerical errors on the potential and the force at  $\beta = 1.00$  on a  $24^4$  lattice with  $N_{\text{tsl}} = 2, 3$ , and  $4$ , where the static charges are separated by the distances along not only on axis but also off axis. Note that the force is computed from the potential by

$$F(r + \frac{h}{2}) = \frac{V(r+h) - V(r)}{h}, \quad (7)$$

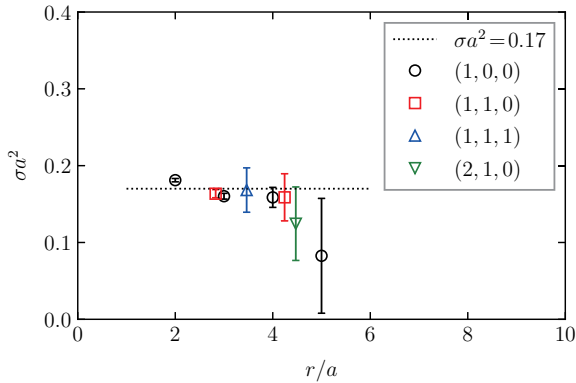


Fig. 5: The direct extraction of the string tension.

where  $h/a = 1$  for the on-axis  $(1, 0, 0)$  data, and  $h/a = \sqrt{2}, \sqrt{3}, \sqrt{5}$  for the off-axis  $(1, 1, 0), (1, 1, 1), (2, 1, 0)$  data, respectively.

Our limited observation suggests that  $N_{\text{tsl}} = 3$  is an optimal choice at  $\beta = 1.00$  among the three. The results with  $N_{\text{tsl}} = 3$  are then plotted in Fig. 4, where the number of internal updates is set to be  $N_{\text{iupd}} = 2000$  with the configurations  $N_{\text{conf}} = 20$ . The standard jack-knife method is used to evaluate the statistical errors. We used the Mac Pro (Late2013) in this computation. In fact, the behavior of the potentials with  $N_{\text{tsl}} = 2$  and with  $N_{\text{tsl}} = 3$  are not so different with each other, but the force exhibits a better behavior with  $N_{\text{tsl}} = 3$ . If one is interested in the long distance behavior of the observables, of course, the number of  $N_{\text{iupd}}$  should be increased. We find that there is no large discrepancy between the data from the on-axis and from the off-axis data, which means that the rotational invariance is reasonably restored at  $\beta = 1.00$ .

The fitting of the potential for the on-axis data to the functional form of a Coulomb and a linear terms,

$$V_{\text{fit}}(r) = -\frac{c}{r} + \sigma r + \mu, \quad (8)$$

gives the values  $c = 0.2363(71)$ ,  $\sigma = 0.1736(27)$ , and  $\mu = 0.5211(96)$  with  $\chi^2/N_{\text{df}} = 1.6$ , where the data in the range  $r/a = [1, 6]$  are taken into account. Similarly, the fitting of the force for the on-axis data to the functional form (derivative of Eq. (8) with respect to  $r$ ),

$$F_{\text{fit}}(r) = \frac{c}{r^2} + \sigma, \quad (9)$$

gives the values  $c = 0.2699(52)$  and  $\sigma = 0.1713(20)$  with  $\chi^2/N_{\text{df}} = 3.2$ , where the data in the range  $r/a = [1.5, 5.5]$  are taken into account. The slope of the linear term  $\sigma$ , which we call the string tension, from Eq. (8) agrees with that from Eq. (9). The small discrepancy in the Coulombic coefficient may reflect a systematic discretization effect.

If the functional form of Eq. (8) is appropriate to describe the behavior of the potential, the string tension can also be extracted by evaluating

$$\sigma = \frac{1}{2} \frac{d^2}{dr^2}(rV(r)), \quad (10)$$

where we take the difference instead of the derivative on the lattice. The result is plotted in Fig. 5. Although the repetition of taking difference of the data increases the numerical error, we observe a plateau around  $\sigma a^2 \sim 0.17$ , which agrees with those from the potential in Eq. (8) and the force in Eq. (9).

#### 4. Summary

We have performed numerical simulation of the U(1) LGT, and have investigated some of basic physical quantities involving the action and the static potential in order to test our numerical code with OpenMP. The peculiar structure of the PDF of the action current density that we have found in the confinement phase indicates that the monopoles surely play an important role for the confinement mechanism. In order to make a quantitative comparison between the U(1) LGT and the DGL theory, we further need to accumulate numerical data. It is also important to discriminate the lattice discretization effect at short distances. The use of the lattice Green function in three dimensions will be helpful for this purpose. As demonstrated in [8] there is a possibility that the dynamics of monopoles can be transformed into a scalar field theory like the Abelian Higgs model. The lattice results will be useful for the quantitative evaluation of such an idea.

The author is grateful to Miho Koma for fruitful collaboration.

[1] Y. Koma, E. M. Ilgenfritz, T. Suzuki and H. Toki, Phys. Rev. D **64**, 014015 (2001)  
 [2] Y. Koma and M. Koma, Phys. Rev. D **95**, 094513 (2017)  
 [3] M. Creutz, L. Jacobs and C. Rebbi, Phys. Rev. D **20**, 1915 (1979)  
 [4] K. J. M. Moriarty, Phys. Rev. D **25**, 2185 (1982)

[5] Y. Koma, M. Koma and P. Majumdar, Nucl. Phys. B **692**, 209 (2004)  
 [6] T. A. DeGrand and D. Toussaint, Phys. Rev. D **22**, 2478 (1980)  
 [7] M. Lüscher, P. Weisz, JHEP **09**, 010 (2001)  
 [8] K. Bardakci and S. Samuel, Phys. Rev. D **18** (1978), 2849